sciendo

Predictive control of a cascade of biochemical reactors

Martin Mojto, Michaela Horváthová, Karol Kiš, Matúš Furka, Monika Bakošová

Slovak University of Technology in Bratislava, Faculty of Chemical and Food Technology, Institute of Information, Engineering, Automation, and Mathematics, Radlinského 9, 812 37 Bratislava, Slovak Republic
martin.mojto@stuba.sk

Abstract: Rapid growth of the human population has led to various problems, such as massive overload of wastewater treatment plants. Therefore, optimal control of these plants is a relevant subject. This contribution analyses control of a cascade of ten biochemical reactors using simulation results with the aim to design optimal and predictive control strategies and to compare the achieved control performance. The plant represents a complicated process with many variables involved in the model structure, reduced to the single-input and single-output system. The first implemented approach is linear offset-free model predictive control which provides the optimal input trajectory minimising a quadratic cost function. The second control strategy is robust model predictive control with similar features as model predictive control but including the uncertainty of the process. The final approach is generalised predictive control, mostly used in the industry because of its simple structure and sufficiently good control performance. All considered predictive controllers provide satisfactory control performance and remove the steady-state control error despite the constrained control inputs.

Keywords: biochemical reactor, generalised predictive control, model predictive control, robust model predictive control, wastewater treatment

Introduction

The term biochemical reactor describes a processing unit supporting a biologically active environment, which involves living organisms or biochemically active substances. If the environmental conditions inside the biochemical reactor are optimal, microorganisms or cells are effectively fulfilling their function without producing impurities. The productivity and growth of microorganisms can be influenced by temperature and the concentration of dissolved gasses, pH value, and nutrients concentration. Therefore, process control of these variables represents an increasingly relevant part of the biotechnology industry (Henson, 2006). Feedback control systems are applied to achieve optimal growth and productivity and to minimise the production costs. The application of process control strategies in biochemical reactors is an important research subject.

The most common industrial controllers are proportional-integration-derivative (PID) controllers. Their simplicity and straightforward application granted them popularity mainly in the chemical and petrochemical industry. In Rajinikanth and Latha (2010), a PID control system was applied to control an unstable biochemical reactor. A PI controller with fractional order filter has been designed for a biochemical reactor in Vinopraba et al. (2013).

The increased availability of online sensors and analysers allowed implementing more advanced optimisation-based controllers to biochemical reactors. An overview of optimal adaptive algorithms applied to chemical and biochemical reactors is presented in Smets et al. (2004). One of the most advantageous optimisation-based techniques is model predictive control (MPC). This approach has been applied in many areas including chemical engineering and food industry. In MPC, dynamic model of a plant is considered to predict its future behaviour. These algorithms can include constraints on process variables. The optimisation-based approach manages to minimise costs and maximise the quality and safety of the operation. Moreover, MPC is very efficient in multivariable control. In Ramaswamy et al. (2005), MPC was considered to control a biochemical reactor towards an unstable steady state tuning prediction horizon to increase control performance of the plant. Nonlinear model predictive control was used to control fed-batch biochemical reactors in Craven et al. (2014) and Chang et al. (2016).

Throughout the years, multiple predictive controllers based on real-time optimal control have been developed. For instance, generalised predictive control (GPC) (Clarke et al., 1987), where the mathematical model is a controlled auto-regressive and integrated moving-average (CARIMA) model. The objective of GPC is to compute a sequence of future

control signals to minimise a multistage cost function. The GPC method in adaptive and nonadaptive configuration was applied to a fed-batch penicillin production in Rodrigues et al. (2002), with the dissolved oxygen concentration as the controlled variable. The GPC in both, adaptive and nonadaptive, configurations improved control performance of the plant compared to the conventional PID and predictive Dynamic Matrix Control. In Akay et al. (2010), the temperature of a biochemical reactor with baker's yeast production was controlled using the GPC approach. The control performance was analysed considering multiple positive and negative step changes of the set point.

The behaviour of biochemical reactors, both continuous and batch, is usually highly nonlinear. In some cases, the nonlinearity may cause process-model mismatch leading to less effective MPC. To overcome this obstacle, robust MPC (RMPC) was implemented. There are many forms of RMPC: e.g., RMPC using linear matrix inequalities (LMIs) was introduced in Kothrare et al. (1996); Lucia and Engell (2013) designed a nonlinear RMPC for a batch biochemical reactor and improved its control performance. RMPC formulated using linear matrix inequalities was designed for a continuously stirred tank reactor (CSTR) in Oravec and Bakošová (2012) and Oravec et al. (2017).

This paper presents the application of various predictive controllers for a cascade of ten biochemical reactors. The considered plant models wastewater treatment removing undesired compounds from water. Optimal control of these devices is a relevant task as sustainability is nowadays one of the key requirements of industrial production. This research aims to compare control performance of conventional MPC, GPC and RMPC implemented to the cascade of ten biochemical reactors using simulations. The control performance was analysed considering various criteria.

Plant Description

The carrousel plants represent an important part of the industrial wastewater treatment technology. Overall, these plants usually consist of several continuous stirred-tank reactors (CSTR) with a large volume. The disadvantage of this industrial unit is the presence of strong disturbances caused by the unstable feed flow rate and wastewater composition (Pons, 2011).

This research considers a cascade of ten aerated biochemical reactors for the carrousel activation shown in Fig. 1 (Derco et al., 1994; Trautenberger, 2017). The given structure of the cascade provides both oxic and anoxic environments for the biomass. Moreover, each bioreactor involves a vertical fan (aerator) and a supply of airflow, to induce the required conditions for the biochemical processes within the cascade. The feed flow (wastewater) characterised by the concentration of the organic component (S) and impurities such as ammonium salts (NH) or nitrates/nitrites (NO) is fed into the first bioreactor of the cascade. The profile of the mixture composition inside the cascade of bioreactors is the following:

- S_0, NH_0, NO_0 (feed flow),
- S_1, NH_1, NO_1 (output from the first bioreactor),
- S_{10}, NH_{10}, NO_{10} (output from the tenth bioreactor).

A part of a mixture from the tenth bioreactor is returned to the first bioreactor as internal reflux and the rest of the mixture enters the final clarifier. The mixture in the final clarifier is separated by the sedimentation process to the effluent and sludge flow. The second (sludge) reflux is produced by the

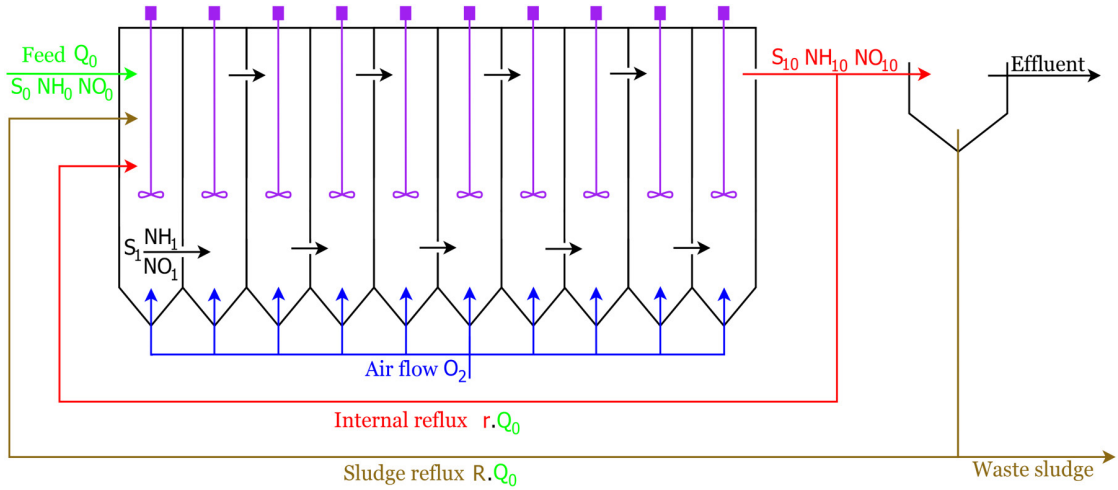

Fig. 1. Flow diagram of the carrousel plant involving the cascade of ten biochemical reactors and a final clarifier.

sludge flow from the clarifier and the rest of the sludge leaves the plant as the waste.

Mass balance equations of the components of the mixture were used to design the mathematical model. These equations follow from the biochemical processes within the plant, such as carbonisation, nitrification, and denitrification. Furthermore, the mathematical model includes the Monod equation to consider the biomass growth. There are several assumptions of the designed mathematical model, such as:

- feed flow without the suspended or solid particles,
- oxygen does not constrain the processes of carbonisation or nitrification,
- reactors inside the cascade are perfectly mixed and variations in the temperature or pH are ignored.

Process identification

The purpose of process identification is to gain desired information about the process dynamics for further analysis (e.g., design of appropriate controllers). The most common structures of the identified models represent a state-space representation or a transfer function. In this case, the identified model represents the transfer function $G(s)$ between:

- the concentration of ammonium salts from the tenth bioreactor (NH_{10}, measured variable and controlled variable in the future),
- the ratio of the internal reflux to the feed flow rate (r, input variable and control input in the future),

in the form of Eq. (1). Since a robust approach was also considered, uncertain parameters were expressed using interval uncertainty within minimal and maximal values of each identified parameter.

The resulting transfer function has the following structure (Furka et al., 2020):

$$G(s) = \frac{b_4 s^4 + b_3 s^3 + b_2 s^2 + b_1 s + b_0}{a_4 s^4 + a_3 s^3 + a_2 s^2 + a_1 s + a_0}, \qquad (1)$$

The numerator is a polynomial of the fourth order with the parameters b_0–b_4 and four zeros. The denominator structure is the same (fourth order polynomial with parameters a_0–a_4) and it involves four poles. The obtained nominal, minimal and maximal values of the transfer function parameters are stated in Tab. 1. The nominal model with nominal values of identified parameters was considered for the design of MPC and GPC. The robust MPC considered vertex systems are models generated for combinations of minimal and maximal values of uncertain parameters. All obtained vertex systems define a convex hull of all possible uncertain systems that represent possible behaviour of the cascade of biochemical reactors. The step response of the process model with nominal, minimal, and maximal parameters is depicted in Fig. 2.

To verify the obtained nominal model of the process, it was compared with the original nonlinear

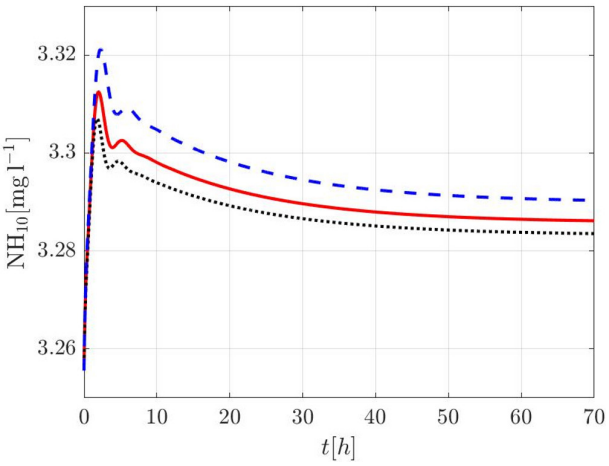

Fig. 2. Step response of the process model with nominal (red solid line), minimal (black dotted line), and maximal (blue dashed line) parameters.

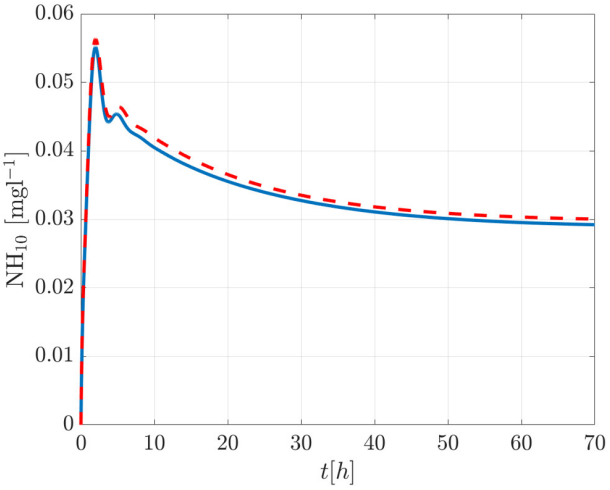

Fig. 3. Comparison of the step response of the nonlinear process (red dashed line) and the identified nominal model (blue solid line).

Tab. 1. Nominal, maximal, and minimal values of identified model parameters.

Parameters	b_0	b_1	b_2	b_3	b_4	a_0	a_1	a_2	a_3	a_4
Nominal	0.03	0.83	0.12	0.11	-56.10^{-3}	0.94	16.77	9.94	5.72	1.00
Maximal	0.04	1.03	0.13	0.11	-54.10^{-3}	1.29	23.06	12.28	6.39	1.00
Minimal	0.02	0.65	0.11	0.10	-52.10^{-3}	0.63	11.24	7.74	5.05	1.00

process (Fig. 3). As it can be seen, the discrepancy (e.g. sum of squared residuals) between the trajectories is negligible. Therefore, the nominal model describes the behaviour of the nonlinear plant sufficiently.

The obtained nominal system can be discretised and transformed to the state-space representation. This form of the model structure is more accessible for the design of controllers. Considering the process dynamics, sampling time $T_s = 0.5$ h is used for discretisation.

Predictive Control Methods

Model predictive control

The cascade of ten biochemical reactors represents a complex system with disturbances and uncertainties. To control this system, linear offset-free MPC was designed and to ensure offset-free control of the plant, augmented model with constant output disturbances was considered (Meader at al., 2009). The augmented state-space model was considered as follows:

$$x(k+1) = Ax(k) + Bu(k),\ x(0) = x_0 \tag{2}$$

$$y(k) = Cx(k) + Fp(k), \tag{3}$$

where $k \geq 0$ is a discrete time instant, $x(k) \in \mathbb{R}^{n_x}$ represents states, $u(k) \in \mathbb{R}^{n_u}$ represents control inputs, $y(k) \in \mathbb{R}^{n_y}$ stands for system outputs and $p(k) \in \mathbb{R}^{n_p}$ stands for constant output disturbances. Parameter x_0 represents the initial conditions of the system. Furthermore, the discrete state-space representation contains matrices $A \in \mathbb{R}^{n_x \times n_x}$, $B \in \mathbb{R}^{n_x \times n_u}$, $C \in \mathbb{R}^{n_y \times n_x}$, $F \in \mathbb{R}^{n_y \times n_p}$ representing state, input, output, and disturbance matrices, respectively.

Based on optimisation, MPC evaluates a sequence of optimal control inputs at each sampling time. The evaluation considers future behaviour of the model and constraints of outputs, inputs, and states. After the evaluation of the sequence of optimal control inputs, MPC considers only the first computed control input to ensure its predictive properties. The optimisation problem is formulated in the following way:

$$\min_{\Delta u(k)} \sum_{k=0}^{N} \left(Q \,\|\, r(k) - y(k) \,\|_2^2 - R \,\|\, \Delta u(k) \,\|_2^2 \right), \tag{4}$$

s.t. $$x(k+1) = Ax(k) + Bu(k),\ x(0) = x_0 \tag{5}$$

$$y(k) = Cx(k) + Fp(k), \tag{6}$$

$$u_{\min} \leq u(k) \leq u_{\max}, \tag{7}$$

$$x_{\min} \leq x(k) \leq x_{\max}, \tag{8}$$

$$y_{\min} \leq y(k) \leq y_{\max}, \tag{9}$$

Parameter N represents the prediction horizon, $r(k) \in \mathbb{R}^{n_y}$ is the reference, $\Delta u(k) = u(k) - u(k-1)$ is the difference of control action. Variables Q and R are tuning matrices weighting control output and control input. The tuning matrices are positively definite and diagonal.

Robust model predictive control

The plant-model mismatch is treated in the RMPC design. The objective of RMPC design is to optimise the state-feedback control law to compute optimal control action. Unlike conventional MPC, RMPC minimises the "worst case" scenario in an infinite cost function horizon at each sampling time. The convex optimisation problem is formulated involving LMIs. In receding horizon setup, RMPC computes the sequence of optimal control actions over the prediction horizon but implements only the first optimal control action. In order to remove steady-state tracking error, $e(k)$, the vector of states was extended by an integral action in the following way:

$$\tilde{x}(k) = \begin{bmatrix} x(k) \\ \sum_{j=0}^{k} e(j) \end{bmatrix},\ e(k) = r(k) - y(k). \tag{13}$$

The extended uncertain state-space model is defined as follows:

$$\tilde{x}(k+1) = \tilde{A}\tilde{x}(k) + \tilde{B}u(k),\ \tilde{x}(0) = \tilde{x}_0 \tag{14}$$

$$y(k) = \tilde{C}\tilde{x}(k), \tag{15}$$

where $\tilde{A}$, $\tilde{B}$, $\tilde{C}$ are matrices of the system extended subject to integral action.

For the purpose of RMPC design, the controlled plant is represented by an uncertain discrete-time state-space model in the following form:

$$\tilde{x}(k+1) = \hat{A}\tilde{x}(k) + \hat{B}u(k),\ x(0) = x_0 \tag{10}$$

$$y = \hat{C}\tilde{x}(k), \tag{11}$$

$$\left[\hat{A}, \hat{B}, \hat{C}\right] \in \operatorname{convhull}\left(\left\{\left[\tilde{A}^{(v)}, \tilde{B}^{(v)}, \tilde{C}^{(v)}\right], \forall v\right\}\right), \quad v \in n_v \tag{12}$$

where v represents the v-th vertex of the system and n_v represents the total number of system vertices.

Input and output symmetric constraints are formulated as Euclidean and peak norms (Kothrare et al., 1996):

$$\begin{gathered} \left\|u(k)\right\|_2 \leq u_{\text{sat}},\ \left|u_j(k)\right| \leq u_{\text{sat},j}, \\ j \in \{1, 2, \ldots, n_u\},\ \left\|y(k)\right\|_2 \leq y_{\text{sat}}, \end{gathered} \tag{16}$$

where u_{sat} and y_{sat} represent values of the symmetric constraints on control inputs and outputs, respectively. However, this approach tends to be conservative as it does not operate with the full range of feasible values of control inputs. To overcome this obstacle, Huang et al. (2011) presented an improved RMPC design method considering the presence of actuator saturation and gain matrix of the state-feedback control law was evaluated without constraints $\tilde{K}(k) \in \mathbb{R}^{n_u \times (n_x + n_y)}$ and with constraints $F(k) \in \mathbb{R}^{n_u \times (n_x + n_y)}$ (Huang et al., 2011). The control input in the presence of actuator saturation, $u_s(k)$ is then computed using the following equation

$$u_s(k) = \left(E_k^m \tilde{K}(k) + \tilde{E}_k^m F_k\right)\tilde{x}(k), \tag{17}$$

where parameter $E_k^m \in \mathbb{R}^{n_u \times n_u}, \quad \forall m \in \{1, \dots 2^{n_u}\}$ is the matrix of all combinations of constrained control inputs. Matrix $\tilde{E}_k^m \in \mathbb{R}^{n_u \times n_u}, \ \forall m \in \{1, \dots 2^{n_u}\}$ represents the matrix of all combinations of unconstrained control inputs.

$$\tilde{E}_k^m = I - E_k^m. \tag{18}$$

The computation of $\tilde{K}(k)$ and $F(k)$ is transformed into the following LMIs

$$\min_{y_k, X_k, Y_k, U_k, Z_k} y_k + \beta y_{s,k} \tag{19}$$

$$\text{s.t.} \quad \begin{bmatrix} X_k & * & * & * \\ \hat{A}^{(v)} X_k + \hat{B}^{(v)} Y_k & X_k & * & * \\ \tilde{Q}^{1/2} X_k & 0 & \gamma_{s,k} I & * \\ R^{1/2} Y_k & 0 & 0 & \gamma_{s,k} I \end{bmatrix} \succcurlyeq 0, \tag{20}$$

$$\begin{bmatrix} X_k & * & * & * \\ \hat{A}^{(v)} X_k + \hat{B}^{(v)} \left(E_k^m Z_k + \tilde{E}_k^m Y_k\right) & X_k & * & * \\ \tilde{Q}^{1/2} X_k & 0 & \gamma_k I & * \\ R^{1/2} \left(E_k^m Z_k + \tilde{E}_k^m Y_k\right) & 0 & 0 & \gamma_k I \end{bmatrix} \succcurlyeq 0, \tag{21}$$

$$\begin{bmatrix} 1 & * \\ \tilde{x}(k) & X_k \end{bmatrix} \succcurlyeq 0, \tag{22}$$

$$\begin{bmatrix} u_{sat}^2 I & * \\ Y_k^T & X_k \end{bmatrix} \succcurlyeq 0, \tag{23}$$

$$\begin{bmatrix} U_k & * \\ Y_k^T & X_k \end{bmatrix} \succcurlyeq 0, \ U_{j,j} \le u_{sat,j}^2, \ j \in \{1, 2, \dots, n_u\}, \tag{24}$$

$$\begin{bmatrix} X_k & * \\ \hat{C}\left[\hat{A}^{(v)} X_k + \hat{B}^{(v)} \left(E_k^m Z_k + \tilde{E}_k^m Y_k\right)\right] & y_{sat}^2 I \end{bmatrix} \succcurlyeq 0, \tag{25}$$

$$\gamma_k - \gamma_{s,k} > 0. \tag{26}$$

Minimisation of auxiliary weight parameter $\gamma_k > 0$ ensures the minimisation of the weighted inverted Lyapunov matrix, X_k, defined as:

$$X_k = \gamma_k P^{-1}, \ P = P^T \succcurlyeq 0. \tag{27}$$

Matrix P represents the Lyapunov matrix. The optimised parameter $\gamma_{s,k} > 0$ shows the weight on unconstrained control input. The weighting constant $\beta > 0$ represents another degree of freedom in the MPC design. Parameters $\tilde{Q} \in \mathbb{R}^{(n_x + n_y) \times (n_x + n_y)}$ and $R \in \mathbb{R}^{n_u \times n_u}$ are weighting matrices. Matrix $\tilde{Q}$ was extended subject to the extended state vector from Eq. (13).

Auxiliary matrix of the controller design without constraints, Z_k is defined as follows:

$$Z_k = \tilde{K} X_k, \tag{28}$$

matrix Y_k represents the auxiliary matrix of the constrained controller design. parameter U_k represents auxiliary matrix of inputs of robust MPC. Symbol * represents the symmetric structure of the matrix, I is the identity matrix of appropriate dimensions and 0 denotes zero matrix of appropriate dimensions.

unconstrained state-feedback controller gain is then computed as follows:

$$\tilde{K} = Z_k X_k^{-1}, \tag{29}$$

constrained state-feedback controller gain is then computed as follows:

$$F = Y_k X_k^{-1}. \tag{30}$$

The considered predictive algorithms (RMPC and MPC) require measurements of the states to compute optimal control input. However, the states of the biochemical reactor considered in this paper were not measurable, therefore the Luenberger state observer was introduced. Detail information on the state observer implementation can be found in Furka et al. (2020).

Generalised predictive control

The considered cascade of ten bioreactors is a SISO system and therefore GPC represents a suitable option for the control of such a plant. This form of the predictive controller is based on the controlled auto-regressive and integrated moving-average (CARIMA) model with the following structure:

$$\alpha(z) y(k) = \beta(z) u(k) + T(z) \frac{d(k)}{\Delta}, \tag{31}$$

where $\alpha(z)$ and $\beta(z)$ are polynomials representing the denominator and numerator of the discrete transfer function for the process:

$$\alpha(z) = 1 + \alpha_1 z^{-1} + \dots + \alpha_n z^{-n}, \tag{32}$$

$$\beta(z) = \beta_1 z^{-1} + \dots + \beta_m z^{-m}, \tag{33}$$

polynomial $T(z)$ explains the behaviour of the disturbances and $d(k)$ is a random variable with zero

mean. The ratio between $d(k)$ and Δ represents slowly varying disturbances.

The advantage of GPC control strategy using the CARIMA model is in unbiased prediction provided by incorporated estimation of disturbances as the previous equation can be transformed to the following incremental form:

$$\alpha(z)\Delta y(k) = \beta(z)\Delta u(k) + T(z)d(k), \tag{34}$$

where $\Delta u(k) = u(k) - u(k-1)$.

Subsequently, products in the previous equation can be modified as follows (Chen, 2013):

$$\begin{aligned} &\textstyle\sum_{i=1}^{n} \alpha_i \Delta y(k+1-i) = \\ &= \textstyle\sum_{i=1}^{n} \beta_i \Delta u(k-i) + \sum_{i=1}^{n} T_i d(k-i). \end{aligned} \tag{35}$$

Prediction of the output can be derived from the left side of Eq. (35):

$$\begin{aligned} &y(k) + \textstyle\sum_{i=1}^{n+1} (\alpha_i - \alpha_{i-1}) y(k-i) = \\ &= \textstyle\sum_{i=1}^{n} \beta_i \Delta u(k-i) + \sum_{i=1}^{n} T_i d(k-i), \end{aligned} \tag{36}$$

where $\alpha_{n+1} = 0$.

This control strategy determines control input minimising the following cost function:

$$J = \left[r(k) - \hat{y}(k)\right]^T Q \left[r(k) - \hat{y}(k)\right] + \Delta u(k)^T R \Delta u(k), \tag{37}$$

where $\hat{y}(k) = G\Delta u(k) + \hat{y}^*(k)$, variables Q and R are tuning matrices and G is a lower-triangular matrix (Clarke et al., 1987).

The output prediction assuming $\Delta u(k) = 0$ is expressed by:

$$\tilde{y}^*(k+j) = H\Phi^j \tilde{x}(k) + H\Phi^{j-1} \Lambda \left[y(k) - H\tilde{x}(k)\right], \tag{38}$$

where the structure of matrices $H\Phi^j$ and $H\Phi^{j-1}$ is shown in (Chen, 2013).

The following structure of input increment can be derived by setting the gradient of Eq. (37) to zero (Grimble, 1992):

$$\begin{aligned} \Delta u(k) &= (G^T Q G + R)^{-1} G^T Q \left[r(k) - \tilde{y}^*(k)\right] = \\ &= K \left[r(k) - \tilde{y}^*(k)\right], \end{aligned} \tag{39}$$

where K is the gain of the controller.

The state-space representation is derived using observable canonical form realisation. The model structure has the following form:

$$x(k+1) = \Phi x(k) + \Gamma \Delta u(k) + \Lambda d(k), \tag{40}$$

$$y(k) = Hx(k) + d(k), \tag{41}$$

matrices Φ, Γ, Λ and H are defined in (Chen, 2013).

The suitable state observer for the designed state-space model (Eq. (40)) is written as:

$$\tilde{x}(k+1) = \Phi \tilde{x}(k) + \Gamma \Delta u(k) + \Lambda \left[y(k) - H\tilde{x}(k)\right]. \tag{42}$$

Results and Discussion

Control setup

The offset-free reference tracking problem was analysed considering a sequence of the step changes of the reference value. The closed-loop control was designed in the MATLAB/Simulink R2019a environment using CPU i7 3.4 GHz and 8 GB RAM.

To formulate optimisation problems of MPC, YALMIP (Löfberg 2004), toolbox was introduced. The optimisation problem of MPC was solved by the GUROBI Optimization (2020). Weighting matrices Q and R and prediction horizon N were tuned as:

$$Q = \begin{bmatrix} 0.01 & 0 & 0 & 0 \\ 0 & 0.01 & 0 & 0 \\ 0 & 0 & 0.01 & 0 \\ 0 & 0 & 0 & 0.01 \end{bmatrix}, \; R = 1, \; N = 30. \tag{43}$$

The constraints on control input were set as follows: $0 \le u(k) \le 60$. Neither the control output, nor the states were constrained during the MPC design.

To formulate robust MPC, MUP toolbox was considered. Semidefinite programming problems (SDPs) were formulated using YALMIP (Löfberg, 2004) and solved by MOSEK (MOSEK ApS., 2019). Variables $\tilde{Q}$ and R were systematically tuned as follows:

$$\tilde{Q} = \begin{bmatrix} 0.01 & 0 & 0 & 0 & 0 \\ 0 & 0.01 & 0 & 0 & 0 \\ 0 & 0 & 0.01 & 0 & 0 \\ 0 & 0 & 0 & 0.01 & 0 \\ 0 & 0 & 0 & 0 & 5 \end{bmatrix}, \; R = 1. \tag{44}$$

The constraints on control input were set as follows: $0 \le u(k) \le 60$. The control output was not constrained during the design of robust MPC.

When designing MPC and RMPC, the Luenberger state observer was considered to augment the state-space from Eq. (2). The disturbance matrix was considered as follows:

$$F = 1. \tag{45}$$

The state-observer used observer gain designed using pole placement in the following way:

$$L = \begin{bmatrix} 0.047 \\ 1.935 \\ -70.218 \\ 300.593 \\ 6.593 \end{bmatrix}. \tag{46}$$

The setup of prediction horizon N and weighting matrices (Q and R) of the GPC control strategy is

the same as in case of MPC (see Eq. (43)). Due to relatively long prediction horizon, it is impractical to display matrix $G \in \mathbb{R}^{N\times N}$ (see Eq. (39)) from the structure of the GPC controller. As it was mentioned before, matrices of the state-space observer (Φ, Γ, Λ and H) were designed according to Chen (2013).

Control performance

The designed predictive controllers were considered to control the plant described by the linear transfer function in Eq. (1). To compare the controllers, two reference step changes were generated, one positive and one negative. The controlled output is depicted in Fig. 4a) and Fig 5a). The corresponding control input is depicted in Fig. 4b) and Fig 5b). All predictive controllers were compared by simulation using the nominal model of the biochemical reactor. To ensure the consistency of the results, similar values of weighting matrices were considered in all predictive methods. The performance of designed control strategies was also compared by integral absolute error (IAE) and integral squared error (ISE). These criteria have the following structures:

$$\mathrm{IAE} = \sum_{k=0}^{150} |e(k)|, \quad \mathrm{IAE} = \sum_{k=0}^{150} e(k)^2, \tag{47}$$

where $e(k)$ is the control error. The resulting values of IAE and ISE criteria are listed in Tab. 2. The obtained values confirm better control performance of MPC, and GPC compared to RMPC.

The resulting trajectories show that all the designed controllers removed the steady-state control error, and each controlled system reached the reference value without offset. Moreover, MPC and RMPC

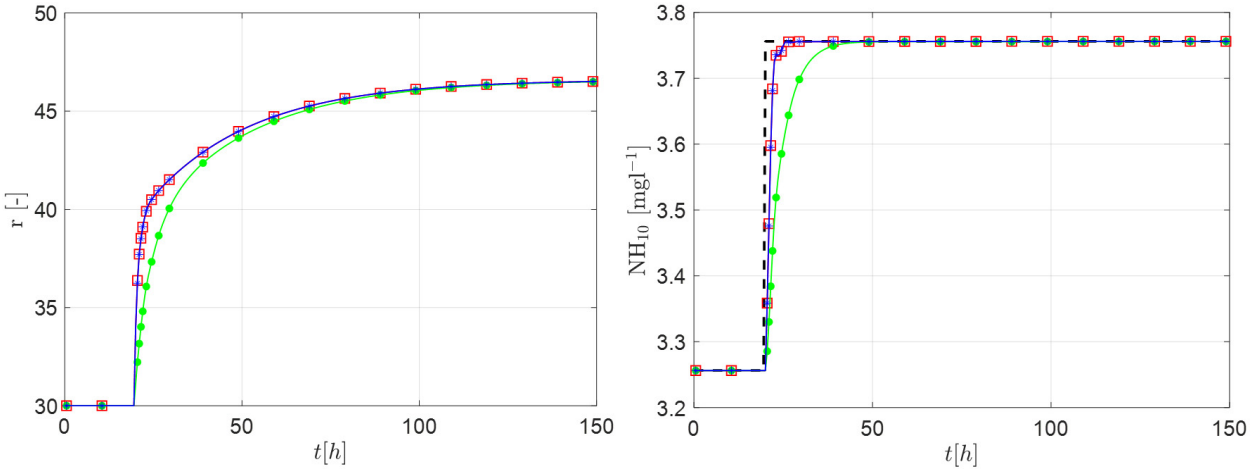

a) Control input to the process b) Output from the process

Fig. 4. Comparison of the control performance provided by positive reference step change. MPC (□), RMPC (●), GPC (*), reference (dashed black) line.

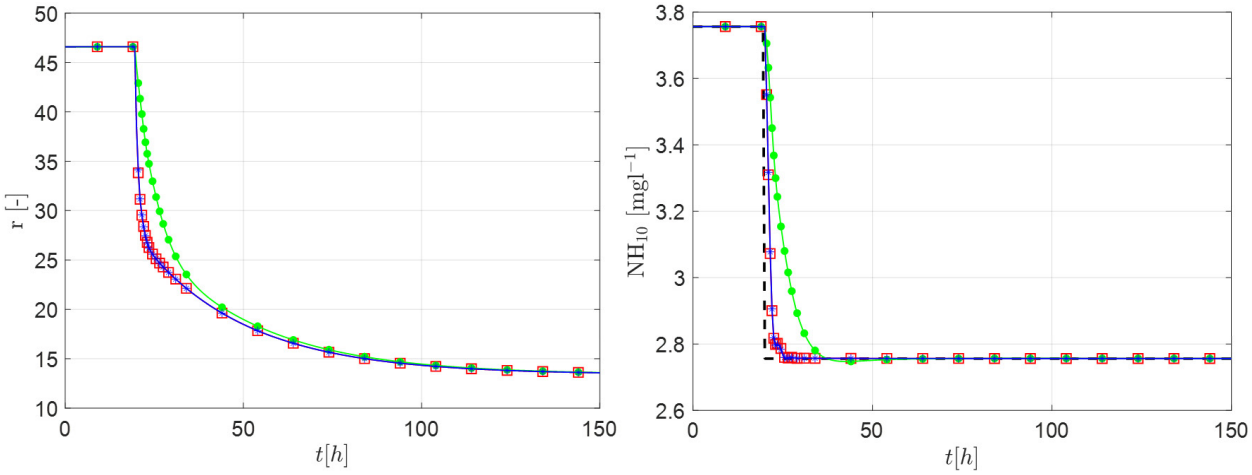

a) Control input to the process b) Output from the process

Fig. 5. Comparison of the control performance provided by negative reference step change. MPC (□), RMPC (●), GPC (*), reference (dashed black) line.

Tab. 2. Comparison of IAE [mg l^{-1} h] and ISE [mg^2 l^{-2} h] criteria of the designed controllers.

Criterion	**IAE [mg l^{-1} h]**			**ISE [mg^2 l^{-2} h]**		
Controller	MPC	RMPC	GPC	MPC	RMPC	GPC
First step change	1.5580	4.7197	1.5594	0.5176	1.2543	0.5205
Second step change	3.1161	9.9396	3.1189	2.0704	5.6376	2.0820
Sum	4.6741	14.6593	4.6783	2.5880	6.8919	2.6025

satisfied the constraints on the control input. The GPC did not consider constraints on the control input during the design.

According to the results, MPC and GPC achieved almost the same control performance. This is mainly caused by the assumption that the controlled process is a single-input-single-output system.

Variations of the feed flow rate represent external disturbance. In the simulation results, variations of the feed flow were considered to be minor and occasional and compensated by a well-tuned controller. If the disturbance is significant, it could be measured to design a control loop with disturbance rejection. Moreover, significant variations of the feed flow rate can still be reduced by storing the feed in additional tank before it enters the carrousel plant.

The output variable of the process (Fig. 4b and 5b) was stabilized faster than the input variable (Fig. 4a and 5a). The reason is the presence of a stable zero in the transfer function of the studied process. All designed controllers try to compensate the effect of this zero and therefore the input variable is still varying while the output variable is already in steady state.

There are also slight differences between the input trajectory of RMPC and of other controllers. This is reflected in the increased settling time and both IAE and ISE criteria. This is an expected result because unlike other controllers, the design of RMPC includes an uncertain model of the plant. If the case study considered control of a nonlinear model, RMPC would be expected to outperform both MPC and GPC, as the process model mismatch would be significant.

Conclusion

In this paper, the design and application of multiple predictive controllers were investigated. The controllers were applied for a cascade of ten biochemical reactors using simulations. First, conventional MPC and GPC were designed for a nominal model of the plant. RMPC was designed, considering an uncertain model of the plant. To design the RMPC, LMI-based approach with reduced conservativeness was applied. The control performance of the designed controllers was compared using integral criteria. As expected, the conventional MPC and GPC control performance was almost identical. Application of the RMPC decreased the control performance; however, this approach is able to handle uncertain and nonlinear behaviour of the plant.

Acknowledgement

The authors gratefully acknowledge the contribution of the Scientific Grant Agency of the Slovak Republic under the grants 1/0585/19 and 1/0545/20, the Slovak Research and Development Agency under the project APVV-15-0007. M. Horváthová was also supported by an internal STU grant.

References

Akay B, Ertunç S, Bursali N, Hapoğlu H, Alpbaz M (2010) Application of generalized predictive control to baker's yeast production, Chemical Engineering Communications, 190: 999—1017.

Chang L, Xinggao L, Henson MA (2016) Nonlinear model predictive control of fed-batch fermentations using dynamic flux balance models, Journal of Process Control, 42: 137—149.

Chen Y (2013) A Novel DMC-Like Implementation of GPC, 2013 International Conference on Mechatronic Sciences, Shenyang, China: 362—366.

Clarke DW, Mohtadi C, Tuffs PS (1987) Generalized predictive control — Part I. The basic algorithm, Automatica, 23: 137—148.

Craven S, Whelan J, Glennon B (2014) Glucose concentration control of a fed-batch mammalian cell bioprocess using a nonlinear model predictive controller, Journal of Process Control, 24: 344—357.

Derco J, Hutňan M, Králik M (1994) Modelling of carrousel type activation (in Slovak), Vodní hospodářství, 42: 23—27.

Furka M, Kiš K, Horváthová M, Mojto M, Bakošová M, (2020) Identification and Control of a Cascade of Biochemical Reactors, 2020, Cybernetics & Informatics, Velké Karlovice, Czech Republic.

Grimble MJ (1992) Generalized predictive optimal control: An introduction to the advantages and limitations, International Journal of System Science 23: 85—98.

GUROBI Optimization (2020) GUROBI Optimizer Quick Start Guide. Version 9.0.

Henson MA (2006) Biochemical reactor modeling and control, IEEE Control Systems Magazine, 26: 54–62.

Huang H, Li D, Lin Z, Xi Y (2011) An improved robust model predictive control design in the presence of actuator saturation, Automatica, 47: 861–864.

Kothare MV, Balakrishnan V, Morari M (1996) Robust constrained model predictive control using linear matrix inequalities, Automatica, 32: 1361–1379.

Löfberg J (2004) YALMIP: A Toolbox for Modeling and Optimization in MATLAB, Proceedings. of the CACSD Conference, Taipei, Taiwan.

Lucia S, Engell S (2013) Robust nonlinear model predictive control of a batch bioreactor using multi-stage stochastic programming, European Control ConfeSCHrence (ECC), Zurich, Switzerland.

MOSEK ApS. (2019) The MOSEK optimization toolbox for MATLAB manual. Version 9.0.

Oravec J, Bakošová M (2012) Robust Constrained MPC Stabilization of a CSTR, Acta Chimica Slovaca, 5: 153–158.

Oravec J, Bakošová M (2015) Software for efficient LMI-based robust MPC design, Proceedings of the 20th International Conference on Process Control, Štrbské Pleso, Slovakia, 272–277.

Oravec J, Bakošová M, Hanulová L, Horváthová M (2017) Design of Robust MPC with Integral Action for a Laboratory Continuous Stirred-Tank Reactor, Proceedings of the 21st International Conference on Process Control, Štrbské Pleso, Slovakia, 459–464.

Pons MN, Mourot G, Ragot J (2011) Modeling and simulation of a carrousel for long-term operation, IFAC World Congress, Milan, Italy.

Rajinikanth V, Latha K (2010) Identification and Control of Unstable Biochemical Reactor, International Journal of Chemical Engineering and Applications, 1: 106–111.

Ramaswamya S, Cutrightb TJ, Qammar HK (2005) Control of a continuous bioreactor using model predictive control, Process Biochemistry, 40: 2763–2770.

Rodrigues JAD, Toledo ECV, Maciel Filho R (2002) A tuned approach of the predictive-adaptive GPC controller applied to a fed-batch bioreactor using complete factorial design, Computers & Chemical Engineering, 26: 1493–1500.

Vinopraba T, Sivakumaran N, Narayanan S, Radhakrishnan TK (2013) Design of fractional order controller for Biochemical reactor, IFAC Proceedings Volumes, 46: 205–208.

Smets IY, Claes JE, November EJ, Georges BP, Van Impe JF (2004) Optimal adaptive control of (bio)chemical reactors: past present and future, Journal of Process Control, 14: 795–805.

Trautenberger R (2017) Modelling and control of a cascade of biochemical reactors, Bachelor Thesis, SCHK, Bratislava, Slovakia.